High Magnetoresistance in Fully Epitaxial Magnetic Tunnel Junctions with a Semiconducting GaO_x Tunnel Barrier

Norihiro Matsuo,[†] Naoki Doko,[†] Tetsuro Takada,[‡] Hidekazu Saito,[*] and Shinji Yuasa

National Institute of Advanced Industrial Science and Technology (AIST), Spintronics Research Center, Umezono 1-1-1, Central 2, Tsukuba, Ibaraki 305-8568, Japan

(Received 7 June 2016; published 21 September 2016)

We fabricate magnetic tunnel junctions with fully epitaxial $Fe(001)/GaO_x(001)/Fe(001)$ structure, where the GaO_x is a wide band-gap semiconductor with a cubic spinel-type crystal structure. Tunneling magnetoresistance ratios up to 92% (125%) are observed at room temperature (20 K), which evidently indicates the existence of a spin-polarized coherent tunneling. The observed MR ratio is the highest among the reported magnetic tunnel junctions with a semiconducting tunnel barrier and ferromagnetic metal electrodes. Such a single-crystalline semiconductor tunnel barrier that shows a high MR ratio is an essential building block for a vertical-type spin field-effect transistor.

DOI: 10.1103/PhysRevApplied.6.034011

I. INTRODUCTION

Magnetoresistance (MR) due to spin-dependent transport in magnetic and nonmagnetic multilayers is an essential physical phenomenon in so-called metal-based spintronics, which has practical applications such as read heads of a hard disk drive, magnetoresistive random access memory, and spin-torque-induced microwave oscillator [1]. The MR effect is also one of the most crucial operation principles in semiconductor-based emerging devices such as spin field-effect transistors (spin FET) [2]. Spin-dependent transport in a semiconductor (SC) is usually studied by using a planar-type device configuration, which has ferromagnetic (FM) source and drain electrodes on a SC channel layer [3–6]. Although highly efficient, spin-dependent transport has recently been demonstrated in such planar devices [7,8], their MR ratios are still too low to meet the requirement for the practical application of spin FET. Here, the MR ratio is defined as $(R_{AP} - R_P)/R_P$ where R_P and R_{AP} are the resistances between the two FM electrodes with parallel and antiparallel magnetization alignments, respectively.

Compared with the planar device configuration, a vertical configuration is of great advantage for achieving a sizable MR. It should be noted that a magnetic tunnel junction (MTJ) [1,9,10], which is the most important practical device in the metal spintronics, is based on the vertical configuration. Recently, there has been some progress in vertical-type SC-based spintronic devices. Kanaki *et al.* [11] fabricated a fully epitaxial vertical-type spin FET with a GaAs channel layer sandwiched between FM semiconductor (Ga, Mn)As source and drain electrodes. They demonstrated the modulations of drain-source current and the MR ratio by applying gate electric fields at a low temperature. Yamada *et al.* [12] and Jenichen *et al.* [13] have successfully grown fully epitaxial metal/SC/metal structure, $Fe_3Si/Ge/Fe_3Si$, which is expected to be applied to the vertical spin FET for room temperature (RT) operation. The vertical structure is also expected to have advantages such as a steep switching behavior and small circuit area compared with the planar structure [11,14]. An epitaxial SC channel is favorable for a high-speed device operation because of its higher carrier mobility than that in polycrystalline or amorphous channels. In MTJs, a fully epitaxial structure is also preferable because the coherent spin-polarized tunneling in fully epitaxial MTJs yields giant MR ratios [1,15–21], which exceeds the limitation in the Julliere's model for diffusive tunneling [22]. To date, giant MR ratios have been observed at RT in fully epitaxial MTJs with insulating barriers such as MgO(001) [19,20] and $MgAl_2O_4(001)$ [21]. *Ab initio* calculations for the epitaxial MTJs with a SC barrier such as ZnSe(001) [15] and GaAs(001) [18] have also revealed very high MR ratios. The giant MR ratio, however, has not been experimentally observed in SC-based MTJs with FM metal electrodes yet [23–31]. Therefore, a new crystalline SC material for the tunnel barrier should be developed.

Gallium oxide (Ga_2O_3) with a band gap (E_g) of ~5 eV has a great potential in various SC devices including FET [32]. This material is known to have several crystal structures, one of which is a cubic $MgAl_2O_4$-type spinel structure (γ phase) [33–36]. It is noteworthy that the lattice constant of γ-Ga_2O_3 (0.824 nm) gives a relatively small lattice mismatch (~1.7%) when the Fe unit cell is turned by 45° with regard to the γ-Ga_2O_3 unit cell in the same manner

[*]Corresponding author.
h-saitoh@aist.go.jp

[†]On leave from Chiba Institute of Technology, 2-17-1 Tsudanuma, Narashino, Chiba 275-0016, Japan.

[‡]On leave from Meiji University, 1-1-1 Higashimita, Tama-ku, Kawasaki, Kanagawa 214-8571, Japan.

as the Fe(001) on $MgAl_2O_4(001)$ [21]. These properties suggest that fully epitaxial Fe(001)/γ-Ga_2O_3(001)/Fe(001) MTJs, which might exhibit a giant MR ratio, can be fabricated. Such MTJs with the γ-Ga_2O_3 barrier nevertheless, have not been reported yet. In this paper, we successfully demonstrate high MR ratios of up to 92% at RT (125% at 20 K) in fully epitaxial MTJs with a γ-$GaO_x(001)$ barrier and Fe(001) electrodes.

II. FILM GROWTH

MTJ films shown in Fig. 1 are prepared by molecular beam epitaxy with electron-beam evaporation. For the growth of the oxide layers, single-crystal Ga_2O_3 and MgO blocks are used as source materials. Crystal structure and surface morphology of each layer during the growth process are monitored by *in situ* reflection high-energy electron diffraction (RHEED). Prior to the growth, the MgO substrate is heated at 800 °C for surface cleaning. Then, an MgO buffer layer and the Fe bottom electrode are, respectively, grown on the substrate at 300 and 100 °C, followed by an *in situ* annealing at 350 °C for 10 min to improve the surface morphology of the Fe bottom electrode. A thin MgO layer with a thickness (d_{MgO}) of 0.4 or 0.7 nm is then epitaxialy grown on the Fe electrode at 100 °C. This MgO acted as a seed layer for the formation of γ-Ga_2O_3 [36] as well as a diffusion barrier between the Fe bottom electrode and the GaO_x layer [37].

A single-crystalline GaO_x tunnel barrier is formed by a solid phase epitaxy technique. A GaO_x layer is first deposited on the MgO insertion layer at 80°C under an O_2 pressure of 1×10^{-6} Torr, which enables us to form a nearly stoichiometric GaO_x ($x \sim 1.5$) layer [38]. No clear diffraction patterns are observed in the RHEED image [Fig. 2(a)], indicating an amorphous GaO_x. Then, an *in situ* annealing is carried out at temperature (T) up to 500 °C with a temperature elevation rate of 20 °C/ min under an O_2 pressure of 1×10^{-7} Torr. Clear streaky patterns appear in the RHEED image after the annealing process [Fig. 2(b)], indicating the formation of a single-crystalline GaO_x with

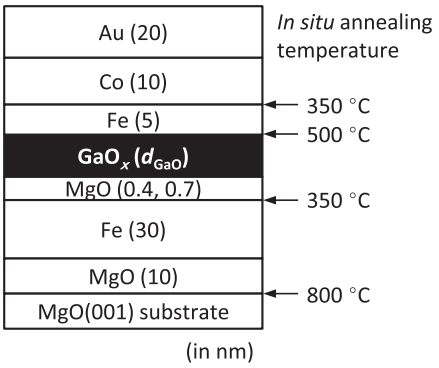

FIG. 1. Structure of the magnetic tunnel junction (MTJ) stack and *in situ* annealing conditions.

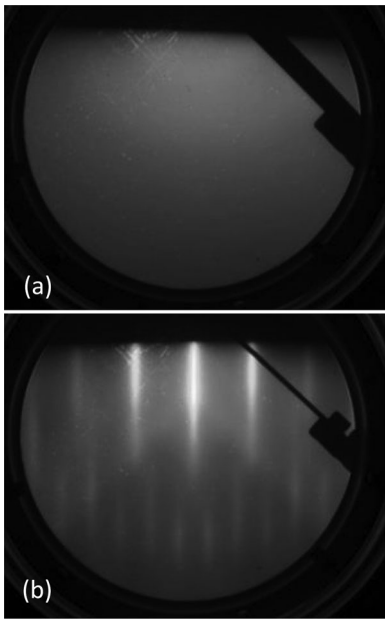

FIG. 2. Reflective high-energy electron diffraction (RHEED) images of the GaO_x layer (a) in the as-grown state and (b) after an *in situ* annealing at 500 °C.

an atomically flat surface. The observed streak patterns have a fourfold symmetry, indicating a cubic crystal structure of the GaO_x layer. Thanks to the single-crystalline barrier, we are able to epitaxially grow the Fe upper electrode, which is grown at 100 °C and then annealed for 10 min at 350 °C to improve the crystalline quality and morphology. Finally, Co-pinned and Au-cap layers are deposited onto the Fe upper electrode at RT. As a reference, we also prepare the same MTJ stack without applying the *in situ* annealing for the GaO_x barrier and the upper Fe electrode to study the difference in magnetotransport properties between the crystal and amorphous GaO_x tunnel barriers. The samples are patterned into tunnel junctions ($3 \times 12\ \mu m^2$) using conventional microfabrication techniques (e.g., photolithography, Ar ion milling, and SiO_2 sputtering).

III. STRUCTURAL ANALYSIS

A cross-sectional scanning transmission electron microscopy (STEM) image [Fig. 3(a)] revealed a fully single-crystal MTJ stack with very few dislocations at the barrier-electrode interfaces or inside the barrier layer. From the STEM image in the range of about 50 nm, the in-plane lattice mismatch $\Delta a/a$ between the barrier and Fe electrodes, is estimated to be between 0.6%–1.0%, where the lattice constant of Fe is smaller. The $\Delta a/a$ value is in reasonable agreement with that expected from the lattice constants of bulk Fe and γ-Ga_2O_3 (~1.7%). The tunnel barrier layer is confirmed to consist of two distinct layers, GaO_x and MgO, from the elemental mapping by energy-dispersive x-ray spectroscopy (EDX). Moreover, no

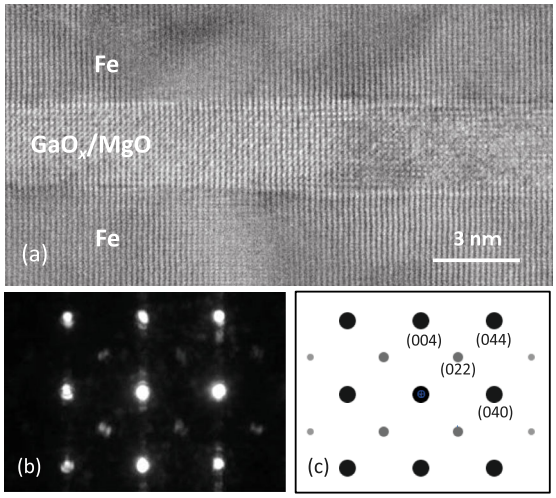

FIG. 3. (a) Cross-sessional bright-field scanning transmission electron microscopy (STEM) image of the MTJ, (b) electron nanobeam diffraction pattern observed in the periphery of the GaO_x layer ([100] azimuth of the MgO substrate), and (c) simulated NBD pattern of a spinel-type $Ga_2O_3(001)$ ([100] azimuth).

diffusion of Fe into the barrier layers is observed [see Figs. 4(a)–4(d)]. As shown in Fig. 3(b), electron nanobeam diffraction (NBD) patterns around the GaO_x layer ([100] azimuth of the MgO substrate) can be assigned as a γ-$Ga_2O_3(001)$ ([100] azimuth) as shown in Fig. 3(c)). Note that other spinel-type compounds such as $FeGa_2O_4$ and $MgGa_2O_4$ cannot be identified by the EDX studies. The epitaxial relations between the electrodes and the barrier layers are determined to be top Fe(001)[110] $||\gamma$-$GaO_x(001)[100]||$ MgO(001)[100] $||$ bottom Fe(001)[110]. From the cross-sectional TEM observations, the thickness of the GaO_x layer (d_{GaO}) after the *in situ* annealing at 500 °C is found to be smaller by 30% than d_{GaO} without the *in situ* annealing process. In this Letter, we therefore use the d_{GaO} value determined from the cross-sectional TEM images of the MTJs.

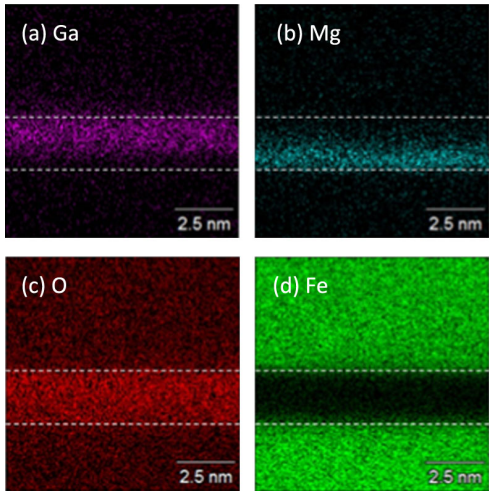

FIG. 4. Elemental mappings of (a) Ga, (b) Mg, (c) O, and (d) Fe $K\alpha$ x-ray lines obtained from the periphery of the GaO_x/MgO layers in the MTJ using energy-dispersive x-ray spectroscopy (EDX). Broken lines indicate the barrier-electrode interface, for guides to the eye.

IV. TRANSPORT PROPERTIES

Figures 5(a) and 5(b), respectively, show typical MR curves of the epitaxial and reference MTJs at $T = 20$ K and RT. The MR ratio is largely enhanced by the *in situ* annealing of the GaO_x barrier. The MR ratio of the epitaxial MTJ is 92% at RT (125% at 20 K), which is a few times larger than those of the reference MTJ (34% at RT and 50% at 20 K) and the highest value reported for FM metal/SC/FM metal MTJs [23–31]. The observed high MR ratio cannot be explained by the Julliere's model with the spin polarization of Fe(001) [39]. The observed large MR ratio is considered to be due to the coherent spin-polarized tunneling in the epitaxial Fe/γ-GaO_x/MgO/Fe MTJs.

Gustavsson *et al.* have measured spin-dependent transport in the fully epitaxial Fe(001)/ZnSe(001)/FeCo(001) MTJs grown by MBE and observed MR ratio up to 16% at 10 K [26]. One of the characteristic phenomena of this MTJ system is a significant reduction of the MR ratio with temperature T. The MR ratio rapidly decreased with

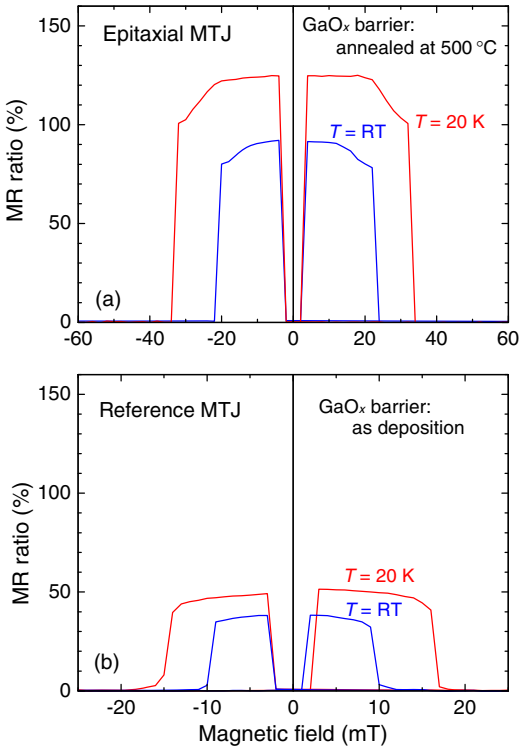

FIG. 5. Typical magnetoresistance (MR) curves of the (a) epitaxial and (b) reference MTJs at 20 K and room temperature (RT) with 5 mV. The total barrier thicknesses are 2.1 nm ($d_{GaO} = 1.7$ nm) for the epitaxial and 2.7 nm ($d_{GaO} = 2.0$ nm) for the reference MTJs.

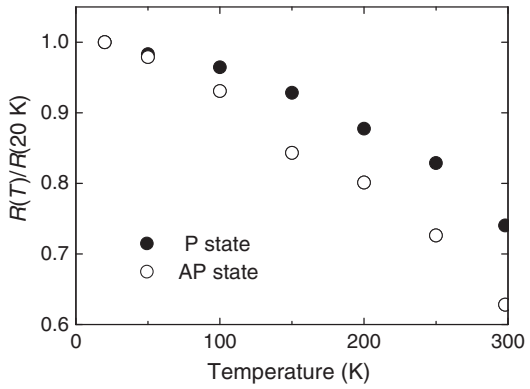

FIG. 6. Relative variations of the junction resistance $R(T)/R(20\ \mathrm{K})$ in the parallel (P) and anti-parallel (AP) states for the epitaxial MTJ shown in Fig. 5(a).

increasing T and vanished above 50 K. This reduction is attributed to the thermally excited carriers in the ZnSe barrier at elevated temperature [26]. In contrast, as indicated in Fig. 5(a), a small variation of the MR ratio as a function T is observed for the present epitaxial MTJs. The relative changes of the MR ratio from RT to 20 K for all the epitaxial MTJs are only 30%–60%, which are comparable to those for the MgO- and $MgAl_2O_4$-based MTJs [19–21]. Furthermore, the MR ratio does not largely depend on the barrier thickness as shown in Fig. 8(a). These results suggest that the epitaxial γ-GaO_x barrier has a much lower number of thermally excited carries at RT compared with those in the ZnSe. To further discuss the results, normalized temperature variations of the junction resistance for the parallel (P) and anti-parallel (AP) states are displayed in Fig. 6. Both values decrease with T, but the variations between 20 K and RT are rather small (35% and 60% for the P and the AP states, respectively). This is consistent with the above-mentioned assumption that there are very few thermally excited carriers in the barrier even at RT. It should be emphasized that this is favorable property for the channel SC of the FET to realize a normally off operation.

Figure 7 shows the bias voltage (V) dependence of the MR ratio for the epitaxial MTJ at RT. The bias V dependence is basically asymmetric. The bias voltages V_{half}, where the MR ratio becomes half of the zero-bias value, are in the range of 450–550 mV at RT regardless of the bias directions and the barrier thicknesses. This implies that there are no significant differences in the crystal quality between the top and bottom electrode-barrier interfaces for all the barrier thicknesses.

The resistance-area (RA) products of the epitaxial MTJs are plotted as a function of the total barrier thickness d_{total} in Fig. 8(b). According to a simple tunnel model [40], the slope of the $\log(RA)$ versus tunnel barrier thickness corresponds to $4\pi(2m\phi)^{1/2}/h$, where h is Plank's constant, m is the free electron mass, and ϕ is the effective barrier height. The slopes the $\log(RA) - d_{\mathrm{total}}$ plot of the GaO_x-based MTJs are close to that reported for the Fe(001)/MgO(001)/Fe(001) MTJs [19], suggesting that the γ-$GaO_x(001)$ has a comparable ϕ value to that of MgO (001) (0.39 eV [19]). It is noteworthy, however, that the RA value decreased with increasing MgO layer thickness in the same d_{total}. This may imply that the density of states of the Fe(001)/GaO_x(001) and Fe(001)/MgO(001) interfaces are considerably different because the intercept of the

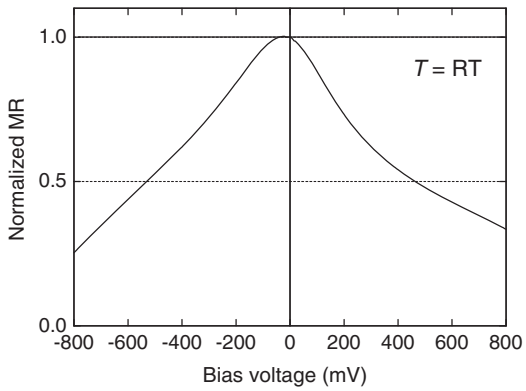

FIG. 7. Bias voltage dependence of normalized MR ratio for the epitaxial MTJ shown in Fig. 5(a) at RT. A positive bias voltage was defined as the bias direction in which the electrons tunnel from the bottom to the top electrodes.

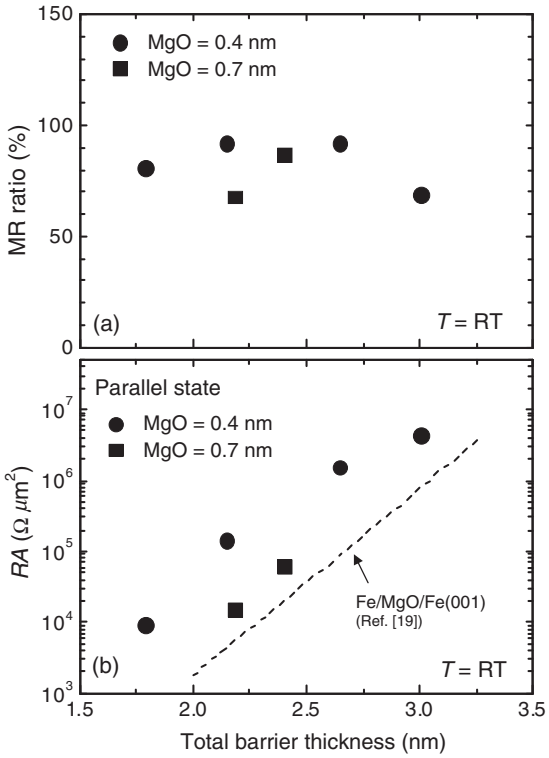

FIG. 8. (a) MR ratio and (b) $\log(RA)$ at RT as a function of the total barrier thickness for the epitaxial MTJs. The RA of the Fe(001)/MgO(001)/Fe(001) MTJs [19] is also shown, for comparison (broken line).

$\log(RA) - d_{\text{total}}$ plot to $d_{\text{total}} = 0$ is expressed by a function of the product of the density of states at the two barrier-electrode interfaces [40]. Another possibly is that the image potential at the barrier-electrode interface [41], which modifies the effective barrier thickness, is different between the Fe(001)/GaO_x(001) and Fe(001)/MgO(001) interfaces.

V. CONCLUSION

We have successfully fabricated fully epitaxial Fe(001)/γ-GaO_x(001)/MgO(001)/Fe(001) MTJs and observed relatively high MR ratios (up to 92% at RT and 125% at 20 K), the highest values reported for FM metal/SC/FM metal MTJs so far. Such high MR ratios indicate the coherent spin-polarized tunneling in the epitaxial MTJs. This result sheds light on a semiconductor as a high-quality tunnel barrier material for the MTJ.

ACKNOWLEDGMENTS

We are grateful to Dr. Key Yakushiji, Dr. Takayuki Nozaki, and Dr. Aurelie Spiesser (AIST) for useful discussions. This work was funded by the ImPACT Program of the Council for Science, Technology and Innovation (Cabinet Office, Government of Japan).

[1] S. Yuasa and D. D. Djayaprawira, Giant tunnel magnetoresistance in magnetic tunnel junctions with a crystalline MgO(0 0 1) barrier, J. Phys. D **40**, R337 (2007).
[2] S. Sugahara and M. Tanaka, A spin metal-oxide-semiconductor field-effect transistor using half-metallic-ferromagnet contacts for the source and drain, Appl. Phys. Lett. **84**, 2307 (2004).
[3] X. Lou, C. Adelmann, S. A. Crooker, E. S. Garlid, J. Zhang, K. S. M. Reddy, S. D. Flexner, C. J. Palmstrøm, and P. A. Crowell, Electrical detection of spin transport in lateral ferromagnet-semiconductor devices, Nat. Phys. **3**, 197 (2007).
[4] O. M. J. van't Erve, A. T. Hanbicki, M. Holub, C. H. Li, C. Awo-Affouda, P. E. Thompson, and B. T. Jonker, Electrical injection and detection of spin-polarized carriers in silicon in a lateral transport geometry, Appl. Phys. Lett. **91**, 212109 (2007).
[5] T. Sasaki, T. Oikawa, T. Suzuki, M. Shiraishi, Y. Suzuki, and K. Tagami, Electrical spin injection into silicon using MgO tunnel barrier, Appl. Phys. Express **2**, 053003 (2009).
[6] Y. Ando, K. Hayama, K. Kasahara, K. Kishi, K. Ueda, K. Sawano, T. Sadoh, and M. Miyao, Electrical injection and detection of spin-polarized electrons in silicon through an Fe_3Si/Si Schottky tunnel barrier, Appl. Phys. Lett. **94**, 182105 (2009).
[7] T. Sasaki, Y. Ando, M. Kameno, T. Tahara, H. Koike, T. Oikawa, T. Suzuki, and M. Shiraishi, Spin Transport in Nondegenerate Si with a Spin MOSFET Structure at Room Temperature, Phys. Rev. Applied **2**, 034005 (2014).
[8] M. Ishikawa, H. Sugiyama, T. Inokuchi, K. Hamaya, and Y. Saito, Spin transport and accumulation in $n+-$Si using Heusler compound Co_2FeSi/MgO tunnel contacts, Appl. Phys. Lett. **107**, 092402 (2015).
[9] T. Miyazaki and N. Tezuka, Giant magnetic tunneling effect in Fe/Al_2O_3/Fe junction, J. Magn. Magn. Mater. **139**, L231 (1995).
[10] J. S. Moodera, L. R. Kinder, T. M. Wong, and R. Meservey, Large Magnetoresistance at Room Temperature in Ferromagnetic Thin Film Tunnel Junctions, Phys. Rev. Lett. **74**, 3273 (1995).
[11] T. Kanaki, H. Asahara, S. Ohya, and M. Tanaka, Spin-dependent transport properties of a GaMnAs-based vertical spin metal-oxide-semiconductor field-effect transistor structure, Appl. Phys. Lett. **107**, 242401 (2015).
[12] S. Yamada, K. Tanikawa, M. Miyao, and K. Hamaya, Atomically controlled epitaxial growth of single-crystalline germanium films on a metallic silicide, Cryst. Growth Des. **12**, 4703 (2012).
[13] B. Jenichen, J. Herfort, U. Jahn, A. Trampert, and H. Riechert, Epitaxial Fe_3Si/Ge/Fe_3Si thin film multilayers grown on GaAs(001), Thin Solid Films **556**, 120 (2014).
[14] H. Takato, K. Sunouchi, N. Okabe, A. Nitayama, K. Hieda, F. Horiguchi, and F. Masuoka, Impact of surrounding gate transistor (SGT) for ultra-high-density LSI's, IEEE Trans. Electron Devices **38**, 573 (1991).
[15] J. M. MacLaren, X.-G. Zhang, W. H. Butler, and X. Wang, Layer KKR approach to Bloch-wave transmission and reflection: Application to spin-dependent tunneling, Phys. Rev. B **59**, 5470 (1999).
[16] J. Mathon and A. Umerski, Theory of tunneling magnetoresistance of an epitaxial Fe/MgO/Fe(001) junction, Phys. Rev. B **63**, 220403R (2001).
[17] W. H. Butler, X.-G. Zhang, T. C. Schulthess, and J. M. MacLaren, Spin-dependent tunneling conductance of Fe|MgO|Fe sandwiches, Phys. Rev. B **63**, 054416 (2001).
[18] P. Mavropoulos, O. Wunnicke, and P. H. Dederichs, Ballistic spin injection and detection in Fe/semiconductor/Fe junctions, Phys. Rev. B **66**, 024416 (2002).
[19] S. Yuasa, T. Nagahama, A. Fukushima, Y. Suzuki, and K. Ando, Giant room-temperature magnetoresistance in single-crystal Fe/MgO/Fe magnetic tunnel junctions, Nat. Mater. **3**, 868 (2004).
[20] S. S. P. Parkin, C. Kaiser, A. Panchula, P. M. Rice, B. Hughes, M. Samant, and S. H. Yang, Giant tunnelling magnetoresistance at room temperature with MgO (100) tunnel barriers Nat. Mater. **3**, 862 (2004).
[21] H. Sukegawa, H. Xiu, T. Ohkubo, T. Furubayashi, T. Niizeki, W. Wang, S. Kasai, S. Mitani, K. Inomata, and K. Hono, Tunnel magnetoresistance with improved bias voltage dependence in lattice-matched Fe/spinel $MgAl_2O_4$/Fe(001) junctions, Appl. Phys. Lett. **96**, 212505 (2010).
[22] M. Julliere, Tunneling between ferromagnetic films, Phys. Lett. **54A**, 225 (1975).
[23] Z. Li, C. de Groot, and J. S. Moodera, Gallium oxide as an insulating barrier for spin-dependent tunneling junctions, Appl. Phys. Lett. **77**, 3630 (2000).
[24] P. Rottländer, M. Hehn, O. Lenoble, and A. Schuhl, Tantalum oxide as an alternative low height tunnel barrier in magnetic junctions, Appl. Phys. Lett. **78**, 3274 (2001).

[25] M. Guth, A. Dinia, G. Schmerber, and H. A. M. van den Berg, Temperature dependence of transport properties in ZnS-based magnetic tunnel junctions, Appl. Phys. Lett. **78**, 3487 (2001).

[26] F. Gustavsson, J. M. George, V. H. Etgens, and M. Eddrief, Structural and transport properties of epitaxial Fe/ZnSe/FeCo magnetic tunnel Junctions, Phys. Rev. B **64**, 184422 (2001).

[27] S. Kreuzer, J. Moser, W. Wegscheider, D. Weiss, M. Bichler, and D. Schuh, Spin polarized tunneling through single-crystal GaAs(001) barriers, Appl. Phys. Lett. **80**, 4582 (2002).

[28] S. S. P. Parkin, Magnetic tunnel junction device with improved insulating tunnel barrier, U.S. Patent No. 6359289 (19 March 2002).

[29] X. Jiang, A. F. Panchula, and S. P. Parkin, Magnetic tunnel junctions with ZnSe barriers, Appl. Phys. Lett. **83**, 5244 (2003).

[30] J. Androulakis, S. Gardelis, J. Giapintzakis, E. Gagaoudakis, and G. Kiriakidis, Indium oxide as a possible tunnel barrier in spintronic devices, Thin Solid Films **471**, 293 (2005).

[31] K. Kobayashi and H. Akimoto, TMR film and head technology, Fujitsu Sci. Tech. J. **42**, 139 (2006).

[32] S. Fujita, Wide-bandgap semiconductor materials: For their full bloom, Jpn. J. Appl. Phys. **54**, 030101 (2015).

[33] R. Roy, V. G. Hill, and E. F. Osborn, Polymorphism of Ga_2O_3 and the system Ga_2O_3-H_2O, J. Am. Chem. Soc. **74**, 719 (1952).

[34] S. Yoshida, H. Hayashi, A. Kuwabara, F. Oba, K. Matsunaga, and I. Tanaka, Structures and energetics of Ga_2O_3 polymorphs, J. Phys. Condens. Matter **19**, 346211 (2007).

[35] T. Oshima, T. Nakazono, A. Mukai, and A. Ohtomo, Epitaxial growth of γ-Ga_2O_3 films by mist chemical vapor deposition, J. Cryst. Growth **359**, 60 (2012).

[36] M. Mitome, S. Kohiki, T. Nagai, K. Kurashima, K. Kimoto, and Y. Bando, A rhombic dodecahedral honeycomb structure with cation vacancy ordering in a γ-Ga_2O_3 crystal, Cryst. Growth Des. **13**, 3577 (2013).

[37] We could also see clear streak RHEED patterns of the GaO_x layer after the *in situ* annealing even without the MgO seed layer. In this case, however, the junction resistances are too low to conduct a reliable MR measurement. This strongly suggests that the MgO layer acts as an effective diffusion barrier between the Fe bottom electrode and the GaO_x barrier.

[38] S. Watanabe, H. Saito, Y. Mineno, S. Yuasa, and K. Ando, Origin of very low effective barrier height in magnetic tunnel junctions with a semiconductor GaO_x tunnel barrier, Jpn. J. Appl. Phys. **50**, 113002 (2011).

[39] S. Yuasa, T. Sato, E. Tamura, Y. Suzuki, H. Yamamori, K. Ando, and T. Katayama, Magnetic tunnel junctions with single-crystal electrodes: A crystal anisotropy of tunnel magneto-resistance, Europhys. Lett. **52**, 344 (2000).

[40] S. Maekawa, S. Takahashi, and H. Imamura, in *Spin Dependent Transport in Magnetic Nanostructures*, edited by S.Maekawa and T.Shinjo (Taylor & Francis, London, 2002), Chap. 4, p. 150.

[41] N. D. Lang and W. Kohn, Theory of metal surfaces: Induced surface charge and image potential, Phys. Rev. B **7**, 3541 (1973).